(D-Ser2) oxyntomodulin recovers hippocampal synaptic structure and theta rhythm in Alzheimer's disease transgenic mice

From the Contents

Guang-Zhao Yang[1, #], Qi-Chao Gao[2, #], Wei-Ran Li[2], Hong-Yan Cai[3], Hui-Min Zhao[2], Jian-Ji Wang[2], Xin-Rui Zhao[2], Jia-Xin Wang[2], Mei-Na Wu[2], Jun Zhang[4], Christian Hölscher[5], Jin-Shun Qi[2, *], Zhao-Jun Wang[2, *]

Graphical Abstract (D-Ser2) oxyntomodulin may be beneficial for the treatment of Alzheimer's disease
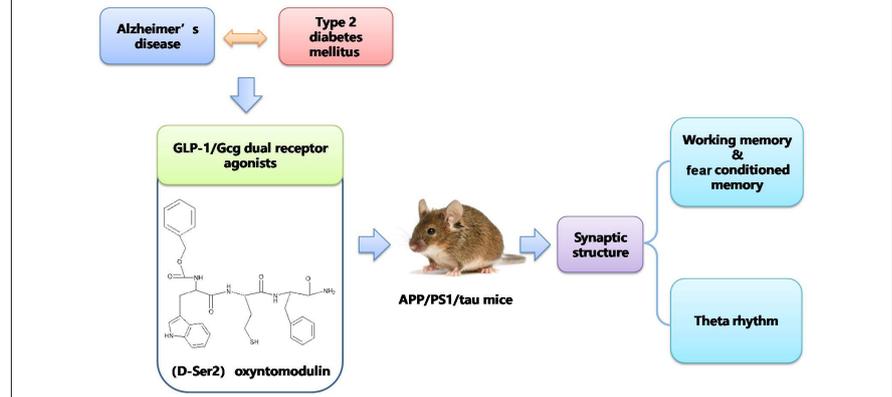
Abstract

In our previous studies, we have shown that (D-Ser2) oxyntomodulin (Oxm), a glucagon-like peptide 1 (GLP-1) receptor (GLP1R)/glucagon receptor (GCGR) dual agonist peptide, protects hippocampal neurons against $A\beta_{1-42}$-induced cytotoxicity, and stabilizes the calcium homeostasis and mitochondrial membrane potential of hippocampal neurons. Additionally, we have demonstrated that (D-Ser2) Oxm improves cognitive decline and reduces the deposition of amyloid-beta in Alzheimer's disease model mice. However, the protective mechanism remains unclear. In this study, we showed that 2 weeks of intraperitoneal administration of (D-Ser2) Oxm ameliorated the working memory and fear memory impairments of 9-month-old 3×Tg Alzheimer's disease model mice. In addition, electrophysiological data recorded by a wireless multichannel neural recording system implanted in the hippocampal CA1 region showed that (D-Ser2) Oxm increased the power of the theta rhythm. In addition, (D-Ser2) Oxm treatment greatly increased the expression level of synaptic-associated proteins SYP and PSD-95 and increased the number of dendritic spines in 3×Tg Alzheimer's disease model mice. These findings suggest that (D-Ser2) Oxm improves the cognitive function of Alzheimer's disease transgenic mice by recovering hippocampal synaptic function and theta rhythm.
Key Words: (D-ser2) oxyntomodulin; Alzheimer's disease; cognitive decline; glucagon-like peptide-1; hippocampus; local field potential; synapse; theta rhythm

Introduction

Alzheimer's disease (AD) is a progressive neurodegenerative disease featuring memory impairment in older people. Global population ageing has led to a rising trend in the prevalence and mortality of AD. However, the pathogenesis of AD has not been fully elucidated (Toricelli et al., 2021). Additionally, effective treatments for AD are still lacking. Many reports indicate that there is a strong pathophysiological link between type 2 diabetes mellitus (T2DM) and AD because of similarities between the pathological mechanisms and characteristics of AD and T2DM (Arnold et al., 2018; Suresh

[1]Department of Cardiovascular Medicine, the First Hospital of Shanxi Medical University, Taiyuan, Shanxi Province, China; [2]Department of Physiology, Shanxi Medical University; Key Laboratory of Cellular Physiology, Ministry of Education; Key Laboratory of Cellular Physiology in Shanxi Province, Taiyuan, Shanxi Province, China; [3]Department of Microbiology and Immunology, Shanxi Medical University, Taiyuan, Shanxi Province, China; [4]Functional Laboratory Center, Shanxi Medical University, Taiyuan, Shanxi Province, China; [5]Research and Experimental Center, Henan University of Chinese Medicine, Zhengzhou, Henan Province, China
*Correspondence to: Zhao-Jun Wang, wzhaojun1025@126.com; Jin-Shun Qi, jinshunqi2009@163.com.
https://orcid.org/0000-0001-7289-5307 (Zhao-Jun Wang); https://orcid.org/0000-0001-9223-8806 (Jin-Shun Qi).
#Both authors contributed equally to this work.

et al., 2021). In recent years, the use of diabetes drugs has been suggested for intervention in AD (Li et al., 2007). Research in this field has attracted increasing attention and has made some progress. For example, insulin receptors have been found to be widely located in the cerebral cortex, hippocampus, and hypothalamus (Graham et al., 2020). Insulin can inhibit the formation of amyloid β (Aβ) and neurofibrillary tangles in the brain and improve neuronal survival (Jagust, 2018). However, desensitization of insulin receptors has been shown in the brains of AD patients (Hölscher, 2020), so the application of insulin in the treatment of AD is not ideal.

In recent years, researchers have looked at other substances that can affect insulin signaling, such as glucagon-like peptide 1 (GLP-1) and other analogues. GLP-1 is a type of intestinal insulin secreted by intestinal cells that can reduce blood glucose and obesity by inhibiting glycemic hormones and controlling appetite in T2DM patients (Haan, 2006; Hamilton et al., 2011; Basalay et al., 2020). Surprisingly, GLP-1 and its analogues also have neuroprotective effects. Many studies have reported that GLP-1 and its analogues can improve various neurodegenerative diseases, including AD and Parkinson's disease (Athauda and Foltynie, 2016; Athauda et al., 2017; Grieco et al., 2019). Recent research in our laboratory has shown that GLP-1 analogues can improve spatial learning and memory, reverse damage to synaptic plasticity, reshape hippocampal synaptic activity, and prevent Aβ-induced intracellular calcium overload in AD animal models (Han et al., 2013; Cai et al., 2018; Li et al., 2018, 2020). Glucagon (Gcg), another important hormone in blood glucose regulation, plays a synergistic role to promote the release of insulin. GLP-1 and Gcg dual receptor channels can cooperate with each other to improve the symptoms of AD animal models (Wang et al., 2020). GLP-1 and Gcg are widely present in the central nervous system. Activation of these two receptors has been demonstrated to have neuroprotective effects (Baggio and Drucker, 2007; Sandoval and D'Alessio, 2015). There is evidence that oxyntomodulin (Oxm), a GLP-1 and Gcg dual receptor agonist, promotes insulin release (Pocai, 2012).

In light of these results, we investigated the neuroprotective effects of (D-Ser2) Oxm, a new Oxm derivative that replaces L-serine (D-Ser) at position 2 of Oxm with Ser. This replacement allows (D-Ser2) Oxm to be protected from degradation by dipeptidase V, thereby increasing its biological half-life (Lynch et al., 2014). Our previous study showed that (D-Ser2) Oxm not only alleviated the impairments of working memory and long-term spatial memory, but also reduced the number of Aβ plaques in the hippocampus of APP/PS1 AD transgenic mice. Moreover, (D-Ser2) Oxm administration significantly increased phosphatidylinositol 3-kinase/phospho-Akt1 (p-PI3K/p-AKT1) expression and decreased phospho-glycogen synthase kinase-3 beta (p-GSK3β) levels in the hippocampus (Wang et al., 2020). These results were the first demonstration of an *in vivo* neuroprotective role of (D-Ser2) Oxm in APPswe/PSEN1dE9 (APP/PS1) mice, which suggested that (D-Ser2) Oxm holds promise for the prevention and treatment of AD.

The brain shares information through synaptic connections, and synaptic plasticity is important for learning and memory formation (Kobayashi et al., 2017). Changes in the postsynaptic structure and dendritic spines of excitatory synapses are considered to be the basis of brain plasticity (Borovac et al., 2018). It follows that the destruction of neural circuits due to synapse loss may lead to the cognitive destruction observed in neurodegenerative diseases such as AD. Synapses are indeed lost in AD, and synapse loss is closely related to the decline of cognitive ability in AD patients (Zhao et al., 2020). It is believed that the plasticity of synaptic structure is important for dementia (Skaper et al., 2017). The formation of dendritic spines in the hippocampus plays an extremely important role in learning and memory. It has been reported that the loss of dendritic spines in some mouse models transfected with Aβ and tau proteins is similar to the synaptic loss observed in AD human patients (Zhuo et al., 2019). Blocking electrical activity leads to a significant decrease in spine size (Harvey et al., 2005), which shows that the spontaneous activity of the neuron is necessary to maintain the physiological spine distribution profile. Recent studies have shown that imbalanced electrical activity may lead to cognitive dysfunction in early AD and has potential as a target of clinical intervention (Woon et al., 2007; Iaccarino et al., 2018).

Considering the above findings, we explored the correlation between behavioral improvement and electrophysiological changes by embedding wireless electrodes into APP/PS1/tau (3×Tg) mice in the present study. Theta rhythms in the hippocampal CA1 local field potential (LFP) during working memory and conditional fear memory activities were recorded simultaneously with behavioral performance. We also examined dendritic spines and synapse-related proteins using Golgi staining and western blot, respectively, to determine the possible mechanism behind the relationship between the behavioral electrophysiology and the synaptic structure in 3×Tg mice.

Materials and Methods

Animals and treatment
Sex differences in the prevalence, risk, and severity of AD have been demonstrated in numerous studies in patients. Additionally, sex differences in neuropathological characteristics and cognitive behaviors have been reported in 3×Tg-AD mice (Yang et al., 2018a) and APP/PS1 mice (Jiao et al., 2016; Laws et al., 2016; Li et al., 2016b). Therefore, to avoid potential effects of sex, only male mice were used in the present study. Twenty male 3×Tg mice (RRID: 004807, Jackson Laboratory, Bar Harbor, ME, USA) and twenty wild-type (WT) mice (C57BL/6J, Experimental Animal Center of Shanxi Medical University, Taiyuan, China; license No. SCXK (Jin) 2019-0007) aged 9 months and weighing 30 ± 5 g were included in the study. Mice were raised in physiological laboratory animal houses at a temperature of 22 ± 2°C, a humidity of 30–50%, and a light/dark cycle of 12/12 hours, during which they were free to drink and eat, and were weighed daily during the experiment.

WT mice were randomly divided into WT + saline and WT + Oxm groups (*n* = 10 per group), and 3×Tg mice were randomly divided into 3×Tg + saline and 3×Tg + Oxm groups (*n* = 10 per group). At 9 months of age, the mice began to receive normal saline (0.1 mL/kg body weight) or (D-Ser2) Oxm (25 nmol/kg body weight) by intraperitoneal injection daily for 2 weeks. (D-Ser2) Oxm was synthesized by Boster (Wuhan, China), and was dissolved in normal saline, then packaged and stored in a refrigerator at −20°C. They continued to receive the daily injections during the behavioral experiments. After behavioral tests, Golgi staining and western blot were performed. All animal experimental procedures were approved by the Institutional Animal Care Committee of Shanxi Medical University (IACUC Issue No. SYDL2021008) and conformed to the guidelines established by the Shanxi Medical University Institutional Animal Care Committee. All experiments were designed and reported according to the Animal Research: Reporting of *In Vivo* Experiments (ARRIVE) guidelines (Percie du Sert et al., 2020).

Wireless multichannel neural recording system
A wireless multichannel neural recording system from Triangle BioSystems International (Durham, NC, USA) was used in this experiment. The system was composed of a 16-channel wireless headstage transmitter, which was installed on the head of the animal and had a rechargeable battery, a receiver/demodulator (NeuroWare), and a computer for data storage and analysis. The effective distance was 5 m. This system allowed us to wirelessly record from the animals while they were awake and moving freely. NeuroWare neural signal acquisition software (Triangle BioSystems International) was used to collect and process LFP signals in real time.

Animal surgery
Mice were anesthetized using isoflurane gas (3% to induce and 1.5% to maintain; Reward, Shenzhen, China). A wireless telemetry recording electrode was surgically implanted in the hippocampal CA1 area using stereotaxic instruments (Reward). The coordinates of the electrode tip were as follows: 2.5 mm posterior to the bregma, 1.8 mm lateral to the midline, and depth of 1.5–1.8 mm. Two reference electrodes were fixed on the opposite sides of skull. The other end of the recording electrode was connected to the amplifier through a rotary interface, and the FPS was monitored during the electrode insertion. A significant theta rhythm after tail-clip stimulation indicated that the electrode had reached the hippocampus (McHugh et al., 1996). At this point, the electrode was fixed to the surrounding skull with dental cement. After the electrode implantation, the recording system was disconnected from the electrode, the wound was disinfected with iodophor after the dental cement was set, and penicillin was injected intraperitoneally to prevent infection. After 7 days of recovery, telemetry data collection and behavioral tests were performed.

Electrical signal acquisition and processing
Before the behavioral experiments, the mice were anesthetized with isoflurane gas, and a rechargeable battery of the wireless transmitter

(Triangle BioSystems International) was affixed to the back of each mouse. The recording electrode was connected to the headstage of the launcher and the power supply was turned on. After the animals were awake for 20 minutes, the NeuroWare neural signal acquisition system was turned on, and the signals were sampled according to the LFP characteristics (sampling frequency: 3000 Hz, bandpass: 0.1–500 Hz) and real-time recording observation.

Y-maze test

The Y-maze was used to assess the working memory of the mice. The Y-maze (Reward) was composed of three arms (30 cm long, 15 cm wide, and 7 cm high) at 120° angles. The mice with electrodes were placed in the middle triangle area facing the same arm and were allowed to move freely for 8 minutes. If the third arm entered was different from the first two, it was considered a correct arm approach. The numbers of total arm entries and correct alternations in the Y-maze were recorded with a camera (Sony, Tokyo, Japan) and Smart 3.0 software system (Panlab, Barcelona, Spain). The percentage of spontaneous alternation = number of correct arm entries/(total number of arm entries − 2) × 100.

Fear conditioning test

We used electric foot shock (LE116, Panlab, Barcelona, Spain) for the fear conditioning test. A pressure-sensing device was installed at the bottom of a box to detect activity. After energy conversion and amplification, the pressure was displayed as a pressure curve changing with time. Using a pressure threshold, the system automatically identified active and freezing states of the mice.

This test included training and testing sessions. In the training session, the mice were allowed to move freely in the training box for 90 seconds without any human interference, and then received 30 seconds of sound stimulation (frequency: 2900 Hz, intensity: 90 dB) as the conditioned stimulus (CS). During the last 2 seconds of the sound stimulation, the mice received a continuous direct current stimulation (current intensity: 0.3 mA, duration: 2 seconds) to their feet. Sound stimulation and direct current stimulation were repeated five times at an interval of 90 seconds. After 24 hours, the testing session was carried out. The mice were placed in a new training box with different colors from the previous training box. The mice were acclimated for 150 seconds. Then, they were given 150 seconds of the CS without the foot shock. The activity and LFP of mice during the CS were recorded. The freezing ratio (freezing time accounts for the percentage of each 30 second-interval) of mice was collected before and during the CS, and the differences between the groups were compared.

Golgi staining

We used Golgi staining to observe the morphology and number of dendritic spines in the hippocampal CA1 region. Golgi staining was performed according to the manufacturer's instructions (FD Rapid Golgi Stain Kit, FD NeuroTechnologies, Inc., Columbia, SC, USA). The brains of mice were quickly removed from the skull without perfusion after the mice were deeply anesthetized with 1% pentobarbital sodium (Shanghai Civic Chemical Technology Co., Ltd. Shanghai, China) via intraperitoneal injection. The brains were then immersed in a solution composed of potassium dichromate, potassium chromate, and mercury chloride, and kept in the dark at room temperature for 2 weeks. Next, the brains were transferred to potassium chromate and stored in the dark for at least 72 hours. Coronal serial sections (100 μm) were cut with a freezing microtome (Leica, Nussloch, Germany). The sections were placed in stronger ammonia water and sodium thiosulfate pentahydrate for 10 minutes, and then rinsed in distilled water twice for 4 minutes each time. Gradient dehydration was performed in 50%, 75%, and 95% ethanol, and the sections were then cleared with dimethylbenzene and mounted onto gelatinized slides. The slices were scanned using the ScanScope CS pathological section scanning imaging system (Aperio, Vista, CA, USA). The images were analyzed using ImageJ 18.0 software (Schneider et al., 2012). The spine density was quantified for every 10-μm segment along the entire visible length of the dendrite. At least five neurons from five different tissue sections were chosen for statistical analysis.

Western blot assay

To observe the expression level of synaptic-related proteins, we used western blot to detect the expression of PSD-95 and SYP. After anesthesia by pentobarbital sodium (50 mg/kg) by intraperitoneal injection, the hippocampal CA1 tissue was separated from the brain. Weighing and protein concentration measurements were performed using the bicinchoninic acid protein determination method (Boster).

Protein samples were separated by 10% sodium dodecylsulphate polyacrylamide gel electrophoresis, transferred to a polyvinylidene fluoride membrane (Millipore, Temrculla, CA, USA), and blocked with 5% skim milk powder at room temperature for 2 hours. The membrane was washed, and then incubated with rabbit anti-postsynaptic density protein 95 (PSD-95; 1:1000, Cat# ab76115, Abcam, Cambridge, UK), rabbit anti-synaptophysin (SYP; 1:1000, Cat# D8F6H, Cell Signaling, Bossdun, MA, USA), and rabbit anti-β-tubulin (1:2000, Cat# AC008, ABclonal, Wuhan, China) overnight at 4°C. Finally, the membrane was washed three times with Tris-buffered saline with Tween-20 for 5 minutes each time. Horseradish peroxidase-conjugated affinipure goat anti-rabbit IgG (1:5000, Cat# BA1054, Boster) was added and the membrane was incubated at 4°C for 2 hours, then washed with Tris-buffered saline with Tween-20 three times for 10 minutes each time. Protein expression was detected by electrochemiluminescence. Relative protein expression was analyzed using ImageJ 18.0 software.

Statistical analysis

No statistical methods were used to predetermine sample sizes; however, our sample sizes were similar to those reported in previous publications (Li et al., 2016a; Zhang et al., 2021). No animals or data points were excluded from the analysis. The evaluator was blinded to grouping. SPSS 22.0 (IBM Corp., Armonk, NY, USA) was used for statistical analysis. The data were expressed as mean ± standard error of mean (SEM). The Y-maze, Golgi staining, and western blot data were analyzed by two-way analysis of variance (ANOVA). The fear conditioning test data were analyzed by one-way ANOVA. The least significant difference and *post hoc* Tukey's multiple comparison tests were used to correct for the multiple comparisons between groups. $P < 0.05$ indicates a statistically significant difference. All statistical charts were created using GraphPad Prism 8.02 (GraphPad Software Inc., San Diego, CA, USA).

Results

(D-Ser2) Oxm improves short-term working memory and influences the theta rhythm in 3×Tg mice

To avoid the influence of stress on the following experiments, the Y-maze spontaneous alternation task was performed before the fear conditioning test. Mice have a propensity to enter a new arm to explore the relatively new environment in the maze (Kraeuter et al., 2019). Two-way ANOVA showed that the genotype and treatment had significant main effects (genotype: $F_{(1, 36)} = 46.83$, $P < 0.001$; treatment: $F_{(1, 36)} = 9.018$, $P < 0.01$) and an interaction effect ($F_{(1, 36)} = 21.42$, $P < 0.001$). Tukey's *post hoc* test showed that the correct alternation percentage was significantly decreased from 81.30 ± 2.37% in the WT + saline group to 58.00 ± 2.04% in the 3×Tg + saline group ($P < 0.01$; **Figure 1A**). (D-Ser2) Oxm treatment restored it to 73.50 ± 2.00% ($P < 0.001$, *vs.* 3×Tg + saline group), nearly equal to the level of the WT + saline group. The results suggested a neuroprotective effect of (D-Ser2) Oxm on short-term spatial memory. There was no significant difference between the groups in total arm entries ($F_{(1, 36)} = 0.3231$, $P > 0.05$; **Figure 1B**). These data suggest that the effects of the APP/PS1/tau gene mutation and (D-Ser2) Oxm treatment were not due to a change in locomotor ability.

During the Y-maze task, we recorded changes in the theta rhythm in the four groups (in the central area before entering the right arm). The trend of the theta rhythms in mice entering the correct arm within 5 seconds in the Y-maze was shown in **Figure 1C**. Two-way ANOVA showed that the genotype and treatment had significant main effects (genotype: $F_{(1, 36)} = 20.16$, $P < 0.001$; treatment: $F_{(1, 36)} = 3.435$, $P = 0.0721$) and an interaction effect ($F_{(1, 36)} = 9.549$, $P < 0.05$). Tukey's *post hoc* test showed that the peak power of the theta rhythm was decreased in 3×Tg + saline mice compared with that in WT + saline mice ($P < 0.001$). However, the theta rhythm was improved after treatment with (D-Ser2) Oxm ($P < 0.01$, *vs.* 3×Tg + saline group; **Figure 1C** and **D**). The results showed that (D-Ser2) Oxm improved the short-term working memory and the associated abnormal theta rhythm of the AD model mice.

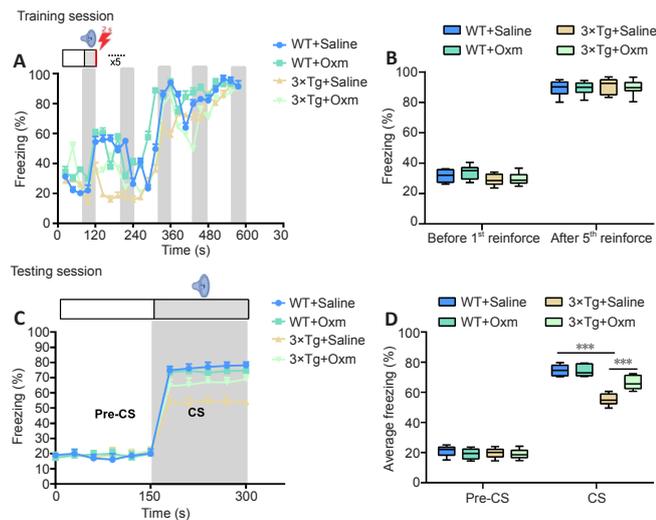### (D-Ser2) Oxm ameliorates fear memory impairment in 3×Tg mice

After the Y-maze experiment, the fear conditioning test was performed. On the first day of fear learning training, as shown in **Figure 2A** and **B**, the freezing ratio increased gradually with the increase of conditioning in all four groups. There were no significant differences in the freezing ratios between the four groups at the beginning or the end of the training ($P > 0.05$), indicating that the APP/PS1/tau gene mutation and (D-Ser2) Oxm had no effect on the

fear learning process. During the testing sessions, the freezing ratio induced by the CS in 3×Tg + saline mice was significantly lower than that in WT + saline mice ($P < 0.001$; **Figure 2C** and **D**). The freezing ratio was improved after (D-Ser2) Oxm treatment ($P < 0.001$, *vs.* 3×Tg + saline group). The above experiments showed that the fear memory of 3×Tg mice was significantly impaired, and was significantly improved after treatment with (D-Ser2) Oxm.
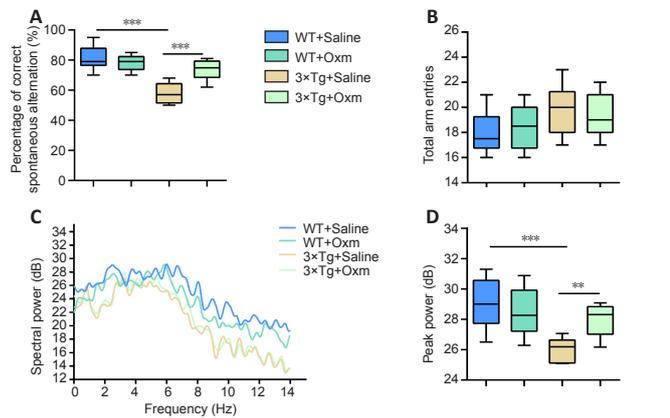
Figure 1 │ **(D-Ser2) Oxm improves working memory and influences theta rhythm in 9-month-old 3xTg mice.**
(A, B) Percentage of correct spontaneous alternation and total arm entries in the Y-maze test. (C) Typical trend of theta rhythm (frequency between 4–10 Hz) in mice entering the correct arm within 5 seconds in the Y-maze. (D) Peak power of theta rhythm within 5 seconds after the mice entered the correct arm in the Y-maze. All values are shown as mean ± SEM ($n = 10$). **$P < 0.01$, ***$P < 0.001$. Statistical comparisons were performed using two-way analysis of variance and *post hoc* Tukey's multiple comparison tests. 3xTg: APP/PS1/tau; Oxm: oxyntomodulin; WT: wild-type.


Figure 2 │ **(D-Ser2) Oxm relieves fear memory impairment in 9-month-old 3xTg mice.**
(A) Freezing ratio during training session of fear conditioning test. (B) Freezing ratio before and after the first reinforcement during the training session. (C) Freezing ratio during the testing session. (D) Freezing ratio before and after conditioned stimulation in the testing session. All values are shown as mean ± SEM ($n = 10$). ***$P < 0.001$ (one-way analysis of variance followed by *post hoc* Tukey's multiple comparison tests). 3xTg: APP/PS1/tau; CS: conditioned stimulus; Oxm: oxyntomodulin; WT: wild-type.

(D-Ser2) Oxm ameliorates the fear memory impairment in 3×Tg mice by increasing theta rhythm power

Figure 3 shows the typical original theta rhythm waveforms, pressure perception curves, and corresponding time-frequency thermograms of the four groups during the testing phase. According to the pressure trace curve, the WT mice were more active in the pre-CS stage, and their activity significantly decreased after CS. The 3×Tg mice showed decreased activity in the CS stage in comparison to the pre-CS stage, and their freezing behavior was decreased compared with that of WT mice after CS. The hippocampal theta rhythm curve

and time-frequency heat map also showed corresponding differences in 3×Tg mice. The freezing state and the power of theta rhythms were improved after treatment with (D-Ser2) Oxm.
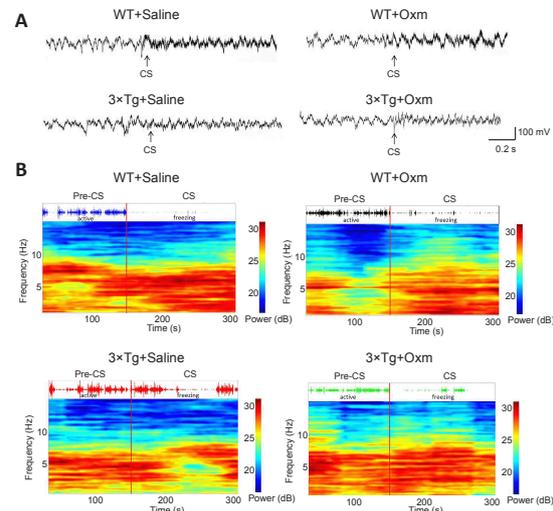
Figure 3 │ **(D-Ser2) Oxm increases the release of the theta waveform, pressure perception curve, and corresponding time-frequency heat map of 9-month-old 3xTg mice between the pre-CS and CS stages.**
(A) The typical original theta waveform. (B) Behavioral electrophysiology recorded simultaneously in the fear box. The upper image is the pressure sensitivity curve and the lower image is the corresponding time-frequency heat map. There was no difference in the release of the theta waveform, pressure perception curve, or corresponding time-frequency heat map of 3xTg mice between the pre-CS and CS stages, and the condition was improved after treatment with (D-Ser2) Oxm. 3xTg: APP/PS1/tau; CS: conditioned stimulus; Oxm: oxyntomodulin; WT: wild-type.

Figure 4A shows the typical peak frequency of the four groups during the testing phase. **Figure 4B** and **C** show the peak frequency and peak power of theta rhythms in the hippocampal CA1 region of mice in each group before and after conditioned stimulation during the fear conditioning test, respectively. The frequency of the theta rhythm in WT + saline mice in the CS stage was higher than that in the pre-CS stage, whereas the theta power in 3×Tg + saline mice was lower than that in WT+ saline mice in the CS phase ($P < 0.001$), which indicated that the fear memory impairment of 3×Tg mice in the CS stage was accompanied by decreased theta power in the hippocampal CA1 region. After (D-Ser2) Oxm treatment, the peak value and frequency of 3×Tg mice in the CS phase were recovered (both $P < 0.001$, *vs.* 3×Tg + saline group). These findings suggested that the fear memory impairment of 3×Tg mice in the CS stage, along with the decreased theta emission power in the hippocampal CA1 region, were improved by (D-Ser2) Oxm treatment.

(D-Ser2) Oxm increases the density of synaptic dendritic spines and the level of synaptic proteins in the hippocampal CA1 region of 3×Tg mice

The synaptic plasticity of the hippocampal CA1 area plays a crucial role in AD cognitive function (Auffret et al., 2009). The above findings demonstrated that (D-Ser2) Oxm improves the working memory and fear memory of 3×Tg mice and the accompanying abnormalities of the theta rhythm. Next, we used Golgi staining to determine whether (D-Ser2) Oxm improves the density of dendritic spines in 3×Tg mice. Two-way ANOVA showed that genotype and treatment had significant main effects on spine density (genotype: $F_{(1, 20)} = 128$, $P < 0.001$; treatment: $F_{(1, 20)} = 55.28$, $P < 0.001$; genotype × treatment: $F_{(1, 20)} = 67.52$, $P < 0.001$). Dendritic spine density in the hippocampal CA1 region of 3×Tg mice was significantly reduced compared with that in the control group ($P < 0.001$), and dendritic spine density was increased in the 3×Tg + Oxm group compared with that in the 3×Tg + saline group ($P < 0.001$; **Figure 5A** and **B**).

PSD-95 and SYP are involved in the regulation of synaptic activity and plasticity (Liu et al., 2018). Two-way ANOVA showed that genotype and treatment had significant main effects on the level of both PSD-95 (genotype: $F_{(1, 20)} = 128$, $P < 0.001$; treatment: $F_{(1, 20)} = 55.28$, $P < 0.001$; genotype × treatment: $F_{(1, 20)} = 67.52$, $P < 0.001$) and SYP (genotype: $F_{(1, 20)} = 62.84$, $P < 0.001$; treatment: $F_{(1, 20)} = 30.24$, $P < 0.001$; genotype × treatment: $F_{(1, 20)} = 13.34$, $P < 0.05$) in the hippocampal

CA1 region. As shown in **Figure 5C–E**, the protein expression levels of PSD-95 and SYP in the hippocampal CA1 region of mice in the 3×Tg + saline group were significantly decreased compared with those in the WT + saline group. Treatment with (D-Ser2) Oxm increased the level of hippocampal synaptic proteins in 3×Tg mice ($P < 0.001$ for each comparison, *vs.* 3×Tg + saline group).
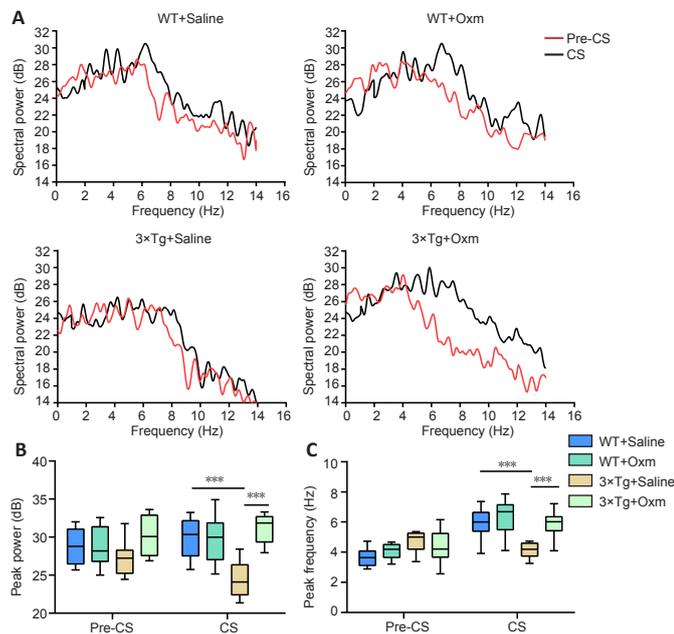
Figure 4 │ **(D-Ser2) Oxm increases the theta power in the hippocampal CA1 of 9-month-old 3xTg mice.**

(A) The peak value of the theta rhythm in the CA1 region was recorded before and after conditioned stimulation during the testing session. In WT + saline mice, the frequency of the theta rhythm in the CS stage was higher than that in the pre-CS stage. (B) Peak power of theta rhythm in CA1 region before and after conditioned stimulation during the testing session. (C) The peak frequency of the theta rhythm in the CA1 region before and after conditioned stimulation during the testing session. All values are shown as mean ± SEM (n = 10). ***$P < 0.001$ (one-way analysis of variance followed by *post hoc* Tukey's multiple comparison tests). 3xTg: APP/PS1/tau; CS: conditioned stimulus; Oxm: oxyntomodulin; WT: wild-type.
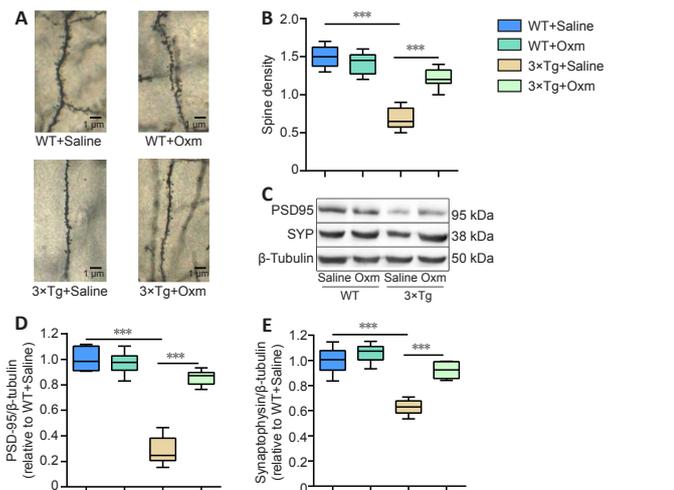
Figure 5 │ **(D-Ser2) Oxm increases the density of dendritic spines and the level of synaptic proteins in the hippocampal CA1 region of 9-month-old 3xTg mice.**

(A) Representative images of dendritic spines in the hippocampal CA1 region of mice. Dendritic spine density was increased in the 3xTg + Oxm group compared with the 3xTg + saline group. Black arrows indicate representative dendritic spines. Scale bars: 1 μm. (B) Dendritic spine density in the hippocampal CA1 area (n = 4). (C) Representative bands showing the expression levels of PSD-95 and SYP in the hippocampus. β-Tubulin was used as a loading control. (D, E) Quantitative analysis of PSD-95 and SYP protein expression (n = 6). All values are shown as mean ± SEM, ***$P < 0.001$. Statistical comparisons were performed using two-way analysis of variance and *post hoc* Tukey's multiple comparison tests. 3xTg: APP/PS1/tau; Oxm: oxyntomodulin; PSD-95: postsynaptic density protein 95; SYP: synaptophysin; WT: wild-type.

Discussion

AD patients experience a progressive decline or loss of memory function in the early stage of the disease. To date, many pathological findings in AD have been reported, including senile plaques with Aβ deposition, neurofibrillary tangles formed by hyperphosphorylated tau protein, and neuroinflammation with extensive involvement of glia. The pathological changes have been associated with cognitive behavior. For example, tau protein phosphorylation is considered to be positively correlated with the degree of dementia in AD patients.

Considering the striking similarity between AD and T2DM in pathogenesis and pathological features, we attempted to use anti-T2DM drugs to treat an animal model of AD. Previous studies in our laboratory have shown that the GLP-1 analogue Val8-GLP-1 prevents $Aβ_{1–40}$-induced spatial learning, memory, and synaptic plasticity damage, remodels hippocampal synaptic activity, and prevents Aβ-induced intracellular calcium overload (Wang et al., 2010, 2013). GLP-1 analogues have been shown to ameliorate spatial learning and memory impairment and the inhibition of hippocampal long-term potentiation in rats (Han et al., 2013; Cai et al., 2014). It has also been reported that the GLP-1 receptor agonist exenatide increases the proliferation of neural stem cells in the brain in diabetic mice (Hamilton et al., 2011) and reduces the level of endogenous Aβ in the brain in AD transgenic mice (Li et al., 2010). Gcg has a synergistic effect with insulin to promote insulin release. Its analogues bind to the receptors on the surface of pancreatic β-cells through peripheral binding, resulting in an increase in intracellular cAMP and calcium concentration, and also promote insulin exocytosis and thus reduce blood glucose in a glucose-dependent manner (Cherrington, 2010). Importantly, GLP-1 and Gcg have a wide range of physiological functions. GLP-1 and Gcg are also highly expressed in many brain regions, including the hippocampus, amygdala, hypothalamus and cerebral cortex (Cork et al., 2015). Expression of GLP-1 and Gcg has also been found in primary cultured hippocampal neurons (Cork et al., 2015). In this study, we found that GLP-1 and Gcg double receptor agonists improved working memory and fear memory and the associated changes of the theta rhythm in 3×Tg mice.

Brain functional activity is expressed through a large number of synaptic connections and is concentrated in the form of regional or global neural network electrical activity. In AD, changes in electrophysiological activity not only accompany the appearance of pathological features, but also may become evident before pathological damage and behavioral disorders. Therefore, some researchers have suggested electroencephalography as a potential means for early diagnosis of AD (Woon et al., 2007). A recent study tried to improve cognitive impairment in AD by changing the characteristic rhythm of brain electrical activity (Iaccarino et al., 2016). However, the neural network activities in different brain regions have their own characteristics and significance. Thus, in the present study, we investigated whether the electrical activity in the hippocampus could be targeted to improve cognitive ability.

The most prominent electrical activity observed in LFP recordings are theta (4–10 Hz) and gamma (30–100 Hz) rhythms. The theta rhythm is mainly generated by the input of the medial septum nucleus, and is very important in the formation and retrieval of plot and spatial memory (Hasselmo, 2005). The theta rhythm of the hippocampus is also related to learning and memory function (Bragin et al., 1995). Brain regions associated with fear memory include the amygdala, medial prefrontal cortex, and hippocampus. The hippocampus is an important structure involved in memory retrieval (Hu et al., 2018). Recent studies have shown that the hippocampus exhibits damage in both neural spines and LFP oscillation activity in AD mice. For example, a previous study performed in our laboratory showed that the theta rhythm is abnormal during the formation of fear memory in 3×Tg mice, indicating that 3×Tg mice have corresponding changes in LFP frequency and power when cognitive abilities are impaired, suggesting that changes in brain electrical activity and changes in behavior are closely related (Yang et al., 2018b). In this study, we found that (D-Ser2) Oxm improved the theta rhythm abnormality in 3×Tg mice. This is consistent with the previous results.

The synapse is an important area of information transmission between neurons. The highly dynamic structure and function of synapses allows for their plasticity. A previous study has reported that (D-Ser2) Oxm directly protects primary hippocampal neurons against $Aβ_{1–42}$-induced cytotoxicity (Han et al., 2016), including cell viability, neuronal apoptosis, mitochondrial membrane potential and intracellular calcium concentration. In this study, the density of

dendritic spines decreased in 3×Tg mice and increased significantly after the administration of (D-Ser2) Oxm. Our findings suggest that (D-Ser2) Oxm improves the synaptic plasticity of 3×Tg mice.

Previous studies have shown that GLP-1 and gastric inhibitory polypeptide play neuroprotective roles in the brain, showing promising effects in AD animal models (Laxton et al., 2010). In this study, the optimized GLP-1 and Gcg dual receptor agonist gastrin modulin (D-Ser2) Oxm significantly improved the theta rhythm associated with working memory and fear memory in 3×Tg mice, and this improvement may be related to synaptic structural plasticity.

Neural information transmission and the realization of brain function are based on the abundant discharge of neurons. Neuron spiking is considered to be fundamental for neural communication. However, this paper only focused on theta rhythms, without analyzing other synchronous electrical activity. We will investigate the relationship between multiple other electrical activity measures and cognitive behavior in future studies.

Taken together, our wireless telemetry behavioral electrophysiology study indicated that (D-Ser2) Oxm ameliorates cognitive deficits and theta rhythm abnormalities, and improves the density of dendritic spines and the expression level of synaptic proteins in 3×Tg mice. Thus, we believe that (D-Ser2) Oxm improves the short-term working memory and fear memory of 3×Tg mice and improves the abnormality of the theta rhythm. In addition, this improvement may be closely related to the plasticity of the synaptic structure.

References

Ansorge MS, Hen R, Gingrich JA (2007) Neurodevelopmental origins of depressive disorders. Curr Opin Pharmacol 7:8-17.

Arnold SE, Arvanitakis Z, Macauley-Rambach SL, Koenig AM, Wang HY, Ahima RS, Craft S, Gandy S, Buettner C, Stoeckel LE, Holtzman DM, Nathan DM (2018) Brain insulin resistance in type 2 diabetes and Alzheimer disease: concepts and conundrums. Nat Rev Neurol 14:168-181.

Athauda D, Foltynie T (2016) The glucagon-like peptide 1 (GLP) receptor as a therapeutic target in Parkinson's disease: mechanisms of action. Drug Discov Today 21:802-818.

Athauda D, Maclagan K, Skene SS, Bajwa-Joseph M, Letchford D, Chowdhury K, Hibbert S, Budnik N, Zampedri L, Dickson J, Li Y, Aviles-Olmos I, Warner TT, Limousin P, Lees AJ, Greig NH, Tebbs S, Foltynie T (2017) Exenatide once weekly versus placebo in Parkinson's disease: a randomised, double-blind, placebo-controlled trial. Lancet 390:1664-1675.

Auffret A, Gautheron V, Repici M, Kraftsik R, Mount HT, Mariani J, Rovira C (2009) Age-dependent impairment of spine morphology and synaptic plasticity in hippocampal CA1 neurons of a presenilin 1 transgenic mouse model of Alzheimer's disease. J Neurosci 29:10144-10152.

Baggio LL, Drucker DJ (2007) Biology of incretins: GLP-1 and GIP. Gastroenterology 132:2131-2157.

Basalay MV, Davidson SM, Yellon DM (2020) Can glucagon-like peptide-1 (GLP-1) analogues make neuroprotection a reality? Neural Regen Res 15:1852-1853.

Borovac J, Bosch M, Okamoto K (2018) Regulation of actin dynamics during structural plasticity of dendritic spines: Signaling messengers and actin-binding proteins. Mol Cell Neurosci 91:122-130.

Bragin A, Jandó G, Nádasdy Z, Hetke J, Wise K, Buzsáki G (1995) Gamma (40-100 Hz) oscillation in the hippocampus of the behaving rat. J Neurosci 15:47-60.

Cai HY, Yang JT, Wang ZJ, Zhang J, Yang W, Wu MN, Qi JS (2018) Lixisenatide reduces amyloid plaques, neurofibrillary tangles and neuroinflammation in an APP/PS1/tau mouse model of Alzheimer's disease. Biochem Biophys Res Commun 495:1034-1040.

Cai HY, Hölscher C, Yue XH, Zhang SX, Wang XH, Qiao F, Yang W, Qi JS (2014) Lixisenatide rescues spatial memory and synaptic plasticity from amyloid β protein-induced impairments in rats. Neuroscience 277:6-13.

Cherrington AD (2010) Glucagon Physiology. Can J Diabetes 34:187-188.

Cork SC, Richards JE, Holt MK, Gribble FM, Reimann F, Trapp S (2015) Distribution and characterisation of Glucagon-like peptide-1 receptor expressing cells in the mouse brain. Mol Metab 4:718-731.

Dean J, Keshavan M (2017) The neurobiology of depression: An integrated view. Asian J Psychiatr 27:101-111.

Duffy AM, Hölscher C (2013) The incretin analogue D-Ala2GIP reduces plaque load, astrogliosis and oxidative stress in an APP/PS1 mouse model of Alzheimer's disease. Neuroscience 228:294-300.

Graham DL, Durai HH, Trammell TS, Noble BL, Mortlock DP, Galli A, Stanwood GD (2020) A novel mouse model of glucagon-like peptide-1 receptor expression: A look at the brain. J Comp Neurol 528:2445-2470.

Grieco M, Giorgi A, Gentile MC, d'Erme M, Morano S, Maras B, Filardi T (2019) Glucagon-like peptide-1: a focus on neurodegenerative diseases. Front Neurosci 13:1112.

Gross C, Zhuang X, Stark K, Ramboz S, Oosting R, Kirby L, Santarelli L, Beck S, Hen R (2002) Serotonin1A receptor acts during development to establish normal anxiety-like behaviour in the adult. Nature 416:396-400.

Haan MN (2006) Therapy Insight: type 2 diabetes mellitus and the risk of late-onset Alzheimer's disease. Nat Clin Pract Neurol 2:159-166.

Hamilton A, Patterson S, Porter D, Gault VA, Holscher C (2011) Novel GLP-1 mimetics developed to treat type 2 diabetes promote progenitor cell proliferation in the brain. J Neurosci Res 89:481-489.

Han WN, Hölscher C, Yuan L, Yang W, Wang XH, Wu MN, Qi JS (2013) Liraglutide protects against amyloid-β protein-induced impairment of spatial learning and memory in rats. Neurobiol Aging 34:576-588.

Han YF, Holscher C, Wang ZJ, Zhang J, Yuan L, Tong JQ, Wang DD, Wu MN, Qi JS (2016) Neuroprotective effects of a novel antidiabetic drug (D-Ser2)Oxm on amyloid β protein-induced cytotoxicity. Sheng Li Xue Bao 68:265-275.

Harvey RJ, Morando L, Rasetti R, Strata P (2005) Spontaneous electrical activity and dendritic spine size in mature cerebellar Purkinje cells. Eur J Neurosci 21:1777-1784.

Hasselmo ME (2005) What is the function of hippocampal theta rhythm?--Linking behavioral data to phasic properties of field potential and unit recording data. Hippocampus 15:936-949.

Hölscher C (2020) Brain insulin resistance: role in neurodegenerative disease and potential for targeting. Expert Opin Investig Drugs 29:333-348.

Hu MM, Yan XD, Zhang XM, Bai Y, Zhao F, Qi JS (2018) Application of wireless neuronal recording system in fear conditioning of Alzheimer's disease mice - hippocampal Theta oscillation observation. Sheng Li Xue Bao 70:571-578.

Iaccarino HF, Singer AC, Martorell AJ, Rudenko A, Gao F, Gillingham TZ, Mathys H, Seo J, Kritskiy O, Abdurrob F, Adaikkan C, Canter RG, Rueda R, Brown EN, Boyden ES, Tsai LH (2016) Gamma frequency entrainment attenuates amyloid load and modifies microglia. Nature 540:230-235.

Iaccarino HF, Singer AC, Martorell AJ, Rudenko A, Gao F, Gillingham TZ, Mathys H, Seo J, Kritskiy O, Abdurrob F, Adaikkan C, Canter RG, Rueda R, Brown EN, Boyden ES, Tsai LH (2018) Author Correction: Gamma frequency entrainment attenuates amyloid load and modifies microglia. Nature 562:E1.

Jagust W (2018) Imaging the evolution and pathophysiology of Alzheimer disease. Nat Rev Neurosci 19:687-700.

Janson J, Laedtke T, Parisi JE, O'Brien P, Petersen RC, Butler PC (2004) Increased risk of type 2 diabetes in Alzheimer disease. Diabetes 53:474-481.

Jiao SS, Bu XL, Liu YH, Zhu C, Wang QH, Shen LL, Liu CH, Wang YR, Yao XQ, Wang YJ (2016) Sex dimorphism profile of Alzheimer's disease-type pathologies in an APP/PS1 mouse model. Neurotox Res 29:256-266.

Kobayashi T, Shimada Y, Fujiwara K, Ikeguchi T (2017) Reproducing infra-slow oscillations with dopaminergic modulation. Sci Rep 7:2411.

Kraeuter AK, Guest PC, Sarnyai Z (2019) The Y-maze for assessment of spatial working and reference memory in mice. Methods Mol Biol 1916:105-111.

Laws KR, Irvine K, Gale TM (2016) Sex differences in cognitive impairment in Alzheimer's disease. World J Psychiatry 6:54-65.

Laxton AW, Tang-Wai DF, McAndrews MP, Zumsteg D, Wennberg R, Keren R, Wherrett J, Naglie G, Hamani C, Smith GS, Lozano AM (2010) A phase I trial of deep brain stimulation of memory circuits in Alzheimer's disease. Ann Neurol 68:521-534.

Li L, Hölscher C (2007) Common pathological processes in Alzheimer disease and type 2 diabetes: a review. Brain Res Rev 56:384-402.

Li L, Liu K, Zhao J, Holscher C, Li GL, Liu YZ (2016a) Neuroprotective role of (Val(8))GLP-1-Glu-PAL in an in vitro model of Parkinson's disease. Neural Regen Res 11:326-331.

Li T, Jiao JJ, Su Q, Hölscher C, Zhang J, Yan XD, Zhao HM, Cai HY, Qi JS (2020) A GLP-1/GIP/Gcg receptor triagonist improves memory behavior, as well as synaptic transmission, neuronal excitability and Ca(2+) homeostasis in 3×Tg-AD mice. Neuropharmacology 170:108042.

Li T, Jiao JJ, Hölscher C, Wu MN, Zhang J, Tong JQ, Dong XF, Qu XS, Cao Y, Cai HY, Su Q, Qi JS (2018) A novel GLP-1/GIP/Gcg triagonist reduces cognitive deficits and pathology in the 3×Tg mouse model of Alzheimer's disease. Hippocampus 28:358-372.

Li X, Feng Y, Wu W, Zhao J, Fu C, Li Y, Ding Y, Wu B, Gong Y, Yang G, Zhou X (2016b) Sex differences between APPswePS1dE9 mice in A-beta accumulation and pancreatic islet function during the development of Alzheimer's disease. Lab Anim 50:275-285.

Li Y, Duffy KB, Ottinger MA, Ray B, Bailey JA, Holloway HW, Tweedie D, Perry T, Mattson MP, Kapogiannis D, Sambamurti K, Lahiri DK, Greig NH (2010) GLP-1 receptor stimulation reduces amyloid-beta peptide accumulation and cytotoxicity in cellular and animal models of Alzheimer's disease. J Alzheimers Dis 19:1205-1219.

Liu Y, Zhang Y, Zheng X, Fang T, Yang X, Luo X, Guo A, Newell KA, Huang XF, Yu Y (2018) Galantamine improves cognition, hippocampal inflammation, and synaptic plasticity impairments induced by lipopolysaccharide in mice. J Neuroinflammation 15:112.

Lynch AM, Pathak N, Flatt YE, Gault VA, O'Harte FP, Irwin N, Flatt PR (2014) Comparison of stability, cellular, glucose-lowering and appetite supressing effects of oxyntomodulin analogues modified at the N-terminus. Eur J Pharmacol 743:69-78.

Mattson MP, Longo VD, Harvie M (2017) Impact of intermittent fasting on health and disease processes. Ageing Res Rev 39:46-58.

McHugh TJ, Blum KI, Tsien JZ, Tonegawa S, Wilson MA (1996) Impaired hippocampal representation of space in CA1-specific NMDAR1 knockout mice. Cell 87:1339-1349.

Mittal K, Katare DP (2016) Shared links between type 2 diabetes mellitus and Alzheimer's disease: A review. Diabetes Metab Syndr 10:S144-149.

Moloney AM, Griffin RJ, Timmons S, O'Connor R, Ravid R, O'Neill C (2010) Defects in IGF-1 receptor, insulin receptor and IRS-1/2 in Alzheimer's disease indicate possible resistance to IGF-1 and insulin signalling. Neurobiol Aging 31:224-243.

Nuzzo D, Picone P, Baldassano S, Caruana L, Messina E, Marino Gammazza A, Cappello F, Mulè F, Di Carlo M (2015) Insulin resistance as common molecular denominator linking obesity to Alzheimer's disease. Curr Alzheimer Res 12:723-735.

Oddo S, Caccamo A, Shepherd JD, Murphy MP, Golde TE, Kayed R, Metherate R, Mattson MP, Akbari Y, LaFerla FM (2003) Triple-transgenic model of Alzheimer's disease with plaques and tangles: intracellular Abeta and synaptic dysfunction. Neuron 39:409-421.

Percie du Sert N, Hurst V, Ahluwalia A, Alam S, Avey MT, Baker M, Browne WJ, Clark A, Cuthill IC, Dirnagl U, Emerson M, Garner P, Holgate ST, Howells DW, Karp NA, Lazic SE, Lidster K, MacCallum CJ, Macleod M, Pearl EJ, et al. (2020) The ARRIVE guidelines 2.0: Updated guidelines for reporting animal research. PLoS Biol 18:e3000410.

Pocai A (2012) Unraveling oxyntomodulin, GLP1's enigmatic brother. J Endocrinol 215:335-346.

Sandoval DA, D'Alessio DA (2015) Physiology of proglucagon peptides: role of glucagon and GLP-1 in health and disease. Physiol Rev 95:513-548.

Schneider CA, Rasband WS, Eliceiri KW (2012) NIH Image to ImageJ: 25 years of image analysis. Nat Methods 9:671-675.

Skaper SD, Facci L, Zusso M, Giusti P (2017) Synaptic plasticity, dementia and Alzheimer disease. CNS Neurol Disord Drug Targets 16:220-233.

Suresh J, Khor IW, Kaur P, Heng HL, Torta F, Dawe GS, Tai ES, Tolwinski NS (2021) Shared signaling pathways in Alzheimer's and metabolic disease may point to new treatment approaches. FEBS J 288:3855-3873.

Talbot K, Wang HY, Kazi H, Han LY, Bakshi KP, Stucky A, Fuino RL, Kawaguchi KR, Samoyedny AJ, Wilson RS, Arvanitakis Z, Schneider JA, Wolf BA, Bennett DA, Trojanowski JQ, Arnold SE (2012) Demonstrated brain insulin resistance in Alzheimer's disease patients is associated with IGF-1 resistance, IRS-1 dysregulation, and cognitive decline. J Clin Invest 122:1316-1338.

Toricelli M, Pereira AAR, Souza Abrao G, Malerba HN, Maia J, Buck HS, Viel TA (2021) Mechanisms of neuroplasticity and brain degeneration: strategies for protection during the aging process. Neural Regen Res 16:58-67.

Walker JM, Harrison FE (2015) Shared neuropathological characteristics of obesity, type 2 diabetes and Alzheimer's disease: impacts on cognitive decline. Nutrients 7:7332-7357.

Wang XH, Li L, Hölscher C, Pan YF, Chen XR, Qi JS (2010) Val8-glucagon-like peptide-1 protects against Aβ1-40-induced impairment of hippocampal late-phase long-term potentiation and spatial learning in rats. Neuroscience 170:1239-1248.

Wang XH, Yang W, Hölscher C, Wang ZJ, Cai HY, Li QS, Qi JS (2013) Val⁸-GLP-1 remodels synaptic activity and intracellular calcium homeostasis impaired by amyloid β peptide in rats. J Neurosci Res 91:568-577.

Wang ZJ, Han YF, Zhao F, Yang GZ, Yuan L, Cai HY, Yang JT, Holscher C, Qi JS, Wu MN (2020) A dual GLP-1 and Gcg receptor agonist rescues spatial memory and synaptic plasticity in APP/PS1 transgenic mice. Horm Behav 118:104640.

Woon WL, Cichocki A, Vialatte F, Musha T (2007) Techniques for early detection of Alzheimer's disease using spontaneous EEG recordings. Physiol Meas 28:335-347.

Yang JT, Wang ZJ, Cai HY, Yuan L, Hu MM, Wu MN, Qi JS (2018a) Sex differences in neuropathology and cognitive behavior in APP/PS1/tau triple-transgenic mouse model of Alzheimer's disease. Neurosci Bull 34:736-746.

Yang Y, Cui Y, Sang K, Dong Y, Ni Z, Ma S, Hu H (2018b) Ketamine blocks bursting in the lateral habenula to rapidly relieve depression. Nature 554:317-322.

Zhang LY, Jin QQ, Hölscher C, Li L (2021) Glucagon-like peptide-1/glucose-dependent insulinotropic polypeptide dual receptor agonist DA-CH5 is superior to exendin-4 in protecting neurons in the 6-hydroxydopamine rat Parkinson model. Neural Regen Res 16:1660-1670.

Zhao J, Fu Y, Yamazaki Y, Ren Y, Davis MD, Liu CC, Lu W, Wang X, Chen K, Cherukuri Y, Jia L, Martens YA, Job L, Shue F, Nguyen TT, Younkin SG, Graff-Radford NR, Wszolek ZK, Brafman DA, Asmann YW, et al. (2020) APOE4 exacerbates synapse loss and neurodegeneration in Alzheimer's disease patient iPSC-derived cerebral organoids. Nat Commun 11:5540.

Zhuo C, Tian H, Li G, Chen M, Jiang D, Lin X, Xu Y, Wang W (2019) Effects of ketamine on circadian rhythm and synaptic homeostasis in patients with treatment-resistant depression: a protocol for mechanistic studies of its rapid and sustained antidepressant actions in humans. Brain Behav 9:e01423.

C-Editor: Zhao M; S-Editors: Yu J, Li CH; L-Editors: McCollum L, Yu J, Song LP; T-Editor: Jia Y